E2-c-Cbl recognition is necessary but not sufficient for ubiquitination activity

Anding Huang[1], Rob N.de Jong[1, 3], Hans Wienk[1], G. Sebastiaan Winkler[2, 3], H.Th.Marc Timmers[2] and Rolf Boelens[1,4]

[1] Department of NMR Spectroscopy, Bijvoet Center for Biomolecular Research, Utrecht University, Padualaan 8, 3584 CH, Utrecht, The Netherlands. [2] Department of Physiological Chemistry, University Medical Center Utrecht, Universiteitsweg 100, 3584 CG, Utrecht, The Netherlands. [3] Current address: Genmab B.V., Yalelaan 60, 3584 CM Utrecht, The Netherlands (R.N.de J.), and school of pharmacy, University of Nottingham, University Park, NG7 2RD Nottingham, U.K. (G.S.W).

[4] Address correspondence to: Phone: +31 30 2534035, Fax: +31 30 2537623, Email: r.boelens@uu.nl

Abstract

The E2 ubiquitin conjugating enzymes UbcH7 and UbcH5B both show specific binding to the RING domain of the E3 ubiquitin-protein ligase c-Cbl, but UbcH7 does not support ubiquitination of c-Cbl and substrate in a reconstituted system. Here, we found that neither structural changes nor subtle differences in the E2-E3 interaction surface are possible explanations for the functional specificity of UbcH5B and UbcH7 in their interaction with c-Cbl. The quick release of ubiquitin from the UbcH5B~Ub thioester to c-Cbl or water suggests that UbcH5B might be a relatively pliable E2 enzyme. In contrast, the UbcH7~Ub thioester is too stable to release ubiquitin to water under our assay conditions, indicating that UbcH7 might be a more specific E2 enzyme. Stronger binding between UbcH7 and the c-Cbl RING domain did not protect c-Cbl from ubiquitination by UbcH5B. Our results imply that the intrinsic enzymatic differences between E2 enzymes contribute to substrate ubiquitination and that the interaction specificity between c-Cbl and E2 is required, but not sufficient for transfer of ubiquitin to potential targets.

Introduction

Post-translational modification by ubiquitin is a major mechanism for regulating protein function in eukaryotes. The general enzymatic cascade of this pathway comprises three enzymes known as E1 (ubiquitin-activating enzyme), E2 (ubiquitin-conjugating enzyme), and E3 (ubiquitin-protein ligase enzyme). The first step in this cascade is the ATP-dependent formation of a thioester bond between ubiquitin and E1, after which ubiquitin is transferred to the catalytic cysteine of an E2 enzyme forming an E2~Ub thioester. Next, the E3 catalyzes the transfer of the ubiquitin from the E2 to a lysine residue of the substrate, with which it forms an isopeptide bond. While HECT domain E3 ligases mediate this step by formation of a HECT-ubiquitin thioester intermediate, RING domain E3 ligases facilitate a direct transfer of ubiquitin from E2 to the substrate via noncovalent interactions with the E2~Ub and the substate (1). In yeast, the substrate can be tagged by a single ubiquitin or ubiquitin chains which can vary in length and linkage specificity. However, only the functions of chains linked through K48 and K63 of ubiquitin have been certainly established. The K48-linked chains are shown to target proteins for degradation via the 26S proteasome, while the K63-linked chains recruit binding partners during inflammation or DNA repair (2).

The E2 enzymes are the key enzymes in the ubiquitin and ubiquitin-like pathways. More than

30 structures of E2s from various organisms are available, and all these E2 proteins share a topologically conserved α/β-fold core domain of ~150 residues. Four α-helices (α1-α4) compose one face of the protein, and a four stranded antiparallel β-sheet (β1-β4) sits on the back of the enzyme between helices α1 and α2 (Figure 4). Every E2 core domain can bind three other proteins: the E1 ubiquitin activating enzyme, a cognate E3 ligase enzyme, and activated ubiquitin via a labile thioester linkage. E2 enzymes can gain additional functionality via association with additional domains or subunits (3,4).

The complex of c-Cbl and UbcH7 was the first RING E3-E2 structure to be solved (5), but further structural insight into E2-E3 interactions comes from the HECT E3 E6-AP complexed to UbcH7 (6), the NMR based model of the RING E3 CNOT4 bound to UbcH5B (7) and the U-box domain E3 CHIP/Ubc13-Uev1a complex (1,8). All these complex structures show equivalent elements in the E2-E3 interface and similarities in overall structure. The core interface is formed by a hydrophobic groove on the E3 and two main regions on the E2: loop L1, located between the strand β3 and β4, and loop L2, connecting the strand β4 and the helix α2. In sharp contrast to the wealth of knowledge on E2 structures, the best structural insight of the E2~Ub thioester intermediate is limited to models based on NMR chemical shift perturbation data due to the inherent instability of the thioester complex (4,9).

The human genome encodes a few E1s (1,10), around 30 E2s, several hundred of E3s and thousands of substrates for ubiquitin, which makes this pathway very versatile and highly complex. An E3 may have more than one substrate and some substrates can be recognized by multiple E3s (11). The large abundance of E3s relative to E2s implies that also E2s can function with multiple E3 ligases, but the inverse situation also exists. For example, the RING E3 complex SCF shows in vitro poly-ubiquitination activity with both CDC34 and Ubc4 (12,13), and the activity of the E3 APC is observed with both UbcH10 and UbcH5A, C (14,15).

It is generally assumed that the binding ability of E2-E3 is the determinant of functional E2-E3 pairs, because decreasing the interaction between E2 and E3 also diminishes their poly- or mono-ubiquitination activity *in vitro*. Interestingly, Brzovic et al. found that the BRCA1/BARD1 E3 heterodimer can interact with UbcH5C and UbcH7 with similar affinity and a similar interface, but only UbcH5C was active in Ub-ligase activity assays (16). Other examples of E3s that can physically interact with some E2s but fail to support ubiquitin transfer to targets include the RING E3 heterodimer Ring1b/Bmr1 (17) and the U-box E3 CHIP (8). These results suggest that binding between E2-E3 pairs does not suffice for function. To address this paradox, we have analyzed and compared the c-Cbl/UbcH5B and c-Cbl/UbcH7 complexes both at a structural and functional level.

The E3 ubiquitin ligases of the Cbl family are key regulators of signaling by many surface receptors. From the N- to C-terminus, c-Cbl contains a tyrosine kinase binding (TKB) domain, a linker region and a RING domain, followed by an extensive proline-rich region and an ubiquitin associated domain (UBA). The UBA domain of Cbl-b, a homolog of c-Cbl, has recently been shown to bind ubiquitin noncovalently, promote Cbl-b UBA dimerization and is required for RTK ubiquitination *in vivo* (18). The RING domain can recruit the E2 and function as an E3 ligase (19). The c-Cbl RING E3 ligase can regulate receptor kinases via their ubiquitin conjugation, and catalyze the ubiquitination of c-Cbl itself as well. Autoubiquitination of E3 enzymes is suggested to represent a regulatory mechanism to control the abundance of Ub protein ligases in cells, since E3 autoubiquitination mediates their

proteasome dependent degradation (20,21). Here, we studied the binding and functional specificity of UbcH5B and UbcH7 to c-Cbl RING using NMR structural analysis, chimeric UbcH5B/UbcH7 proteins and *in vitro* activity assays, mostly by studying autoubiquitination of c-Cbl RING. We found that although both UbcH5B and UbcH7 can bind specifically to c-Cbl RING domain, only UbcH5B can facilitate ubiquitination of c-Cbl and substrate, which suggests that the binding specificity between E2-E3 pairs does not necessarily suffice for their functional specificity.

Methods

Construction of Plasmids

The construct of wild-type human UbcH5B was amplified from a human cDNA library and cloned into the pLICHIS, a pET15B derived expression vector, by Enzyme-free cloning (22). The chimera 7H1, 7L1 and 7L2 (Table 1) plasmids was amplified from the plasmid pLICHIS-UbcH5B, and further details are provided as Supplementary information. The fragment enconding the c-Cbl linker and RING domain (358-437) was cloned from a human cDNA library and into pLISHISGST vector (22). Correct constructions of these plasmids were confirmed by DNA sequencing. The plasmid of UbcH7 was described before (23). The pGEX4T1 expression plasmid containing c-Cbl (47-447) was a kind gift of Dr N.P.Pavletich (Memmorial Sloan-Kettering Cancer Center).

To allow ^{32}P labeling of ubiquitin, a protein kinase A recognition site was introduced in the normal enzyme free cloning short forward 5' and LIC forward 5' primers to generate ^{32}P-labeled Ub-K63, in which all lysine residues were mutated except for K63. PCR A was amplified from pET14b-Ub-K63 vector (kindly provided by Dr R.Baer, Columbia University) with short forward 5' TG*CGTCGTGCATCTGTT*atgcagatcttcgtgaagac and LIC reverse 5'

CAAGAAGAACCCCTCAcccacctctgagacggagt ac. PCR B was performed with LIC forword 5' GCCGCGCGGCAGC*CTGCGTCGTGCATCTG TT*atgcagatcttcgtgaagac and short reverse 5' TCAcccacctctgagacggagtac. The hybridized PCR product of PCR A and B was cloned into pLICHIS vector.

Recombinant Protein Expression and Purification

Overexpression and lysis of ^{15}N and ^{13}C/^{15}N-labeled c-Cbl were accomplished by growing *Escherichia coli* BL21(DE3) Rosetta 2 strains (Novagen) containing the pLICHISGST-Cbl (358-437) expression vector in minimal medium mainly as described before (24), and further details are provided as Supplementary information. Purification was carried out by binding the lysate supernatant to gluthation-agarose (Sigma) in buffer B (50mM KH_2PO_4/K_2HPO_4 pH 7.3, 100mM NaCl, 100μM $ZnCl_2$, 0.2mM PMSF, 5mM DTT), washing with buffer B plus 900mM NaCl, and changing to buffer C (50mM KH_2PO_4/K_2HPO_4 pH 7.3, 100mM NaCl, 100μM $ZnCl_2$, 1mM DTT) for GST cleavage. The GST tag was cleaved on the gluthation-agarose beads by addition of 2 U of thrombin (Sigma) per milligram protein at RT for 1 hr and kept at 4^oC for overnight. Protein was eluted out by buffer B plus 500mM NaCl. Thrombin was inactived by addition of 0.5mM PMSF (final concentration). The c-Cbl sample was exchanged to buffer B and concentrated to final concentration of 1.0-1.2 mM using a 5-kDa cutoff spinconcentrators (Amicon ultra-15).

The unlabeled and ^{15}N-labeled His-tagged UbcH5B and the 7H1, 7L1 and 7L2 chimera were expressed in *Escherichia coli* BL21 (DE3) strain and purified on a Nickel-charged Poros MC column (PerSeptive Biosystems) (24). The overexpression of unlabeled and ^{15}N-labeled GST-UbcH7 in *Escherichia coli* BL21 (DE3) were performed as described (23) and buffer exchanged to buffer B.

NMR spectroscopy and structure calculation

NMR experiments were carried out on Bruker AVANCE 600 and 700 spectrometers equipped with a triple-resonance z-gradient probe. The spectra for resonance assignment and structure determination of c-Cbl (aa 358-437) were recorded by a standard set of NMR experiments (25) at 298 K in a buffer containing 50mM KH_2PO_4/K_2HPO_4 pH 7.3, 100mM NaCl, 100μM $ZnCl_2$, 0.2mM PMSF, 5mM DTT, 95%/5% H_2O/D_2O and a small amount of complex protease inhibitor (Roche). All NMR spectra were processed using XwinNMR3.5 (Bruker) and analyzed using the program SPARKY. Structure calculations were performed using the program CYANA (26). The final structures were validated with WHATIF (27) and PROCHECK (28). Molecular images were generated with PyMol (29).

NMR titrations

Unlabeled UbcH5B and UbcH7 were prepared in buffer B. For the binding titrations, the $[^{15}N-^1H]$-HSQC spectra of 100 μM c-Cbl (358-437) in buffer B were recorded at 298 K alone and in complex with different stoichiometric rations of UbcH5B and UbcH7 (1:0.25 to 1:1.5). Combined chemical shift perturbations were calculated using the equation, $\Delta\delta ppm=((\Delta\delta HN)^2+(\Delta\delta N/5)^2)^{1/2}$. The chemical shift changes were plotted against the molar ratio of Ubc:c-Cbl and fitted to standard 1:1 binding curves using Origin 7.0. For the reciprocal binding titrations, ^{15}N-labeled UbcH5B and UbcH7 were prepared in buffer B at a concentrationof 100 μM, and c-Cbl was added to them until a final ratio of c-Cbl:Ubc=2:1. The ^1H and ^{15}N backbone assignments of UbcH5B and UbcH7 were from Biological Magnetic Resonance Data Bank (BMRB) entries 6277 and entry 15498 (30,31) respectively.

^{32}P Labeling of Ubiquitin

pLICHIS-Ub-K63 containing an N-terminal His-tag and Protein Kinase A site was expressed in *E.coli* BL21 (DE3). Purified ubiquitin was labeled in a 100μL reaction containing 4 μL $[\gamma^{32}P]$-ATP, 4 μL PKA (5U/μl, Sigma P2645), 40-80 μg protein in buffer 20mM Hepes/KOH pH 7.5, 100mM NaCl, 12mM $MgCl_2$ and 1mM DTT. After 30 min incubation at 30^oC, ^{32}P-Ubiquitin was purified using magnetic N-beads (Promega) to separate radiolabeled protein from free label.

Enzyme assays (In vitro Ubiquitination assay and thioester release assay)

The standard reactions (15 μl) of E2~Ub thioester formation assay contained 50ng E1, 0.5μM-10μM E2, $1*10^4$ cpm ^{32}P-Ub in a buffer 50mM Tris-HCl pH7.5, 50mM NaCl, 5mM $MgSO_4$, 5mM ATP, and incubated for 30 min at 30^oC. For the c-Cbl autoubiquitination assay, 4 μM c-Cbl (358-437) or c-Cbl (47-447) was added in the reactions and incubated for 90min. In the competition assay, the indicated amounts of UbcH5B, UbcH7 and c-Cbl were included in the E2 activity reaction. For the release assays, 0.2 unit/μl apyrase was added to deplete ATP after the E2~Ub thioester formation assay. Samples were taken out at the indicated times, stopped by adding reducing or nonreducing SDS sample buffer, separated by 12% SDS-PAGE and subjected to autoradiography.

Results

Ub-charged UbcH7 cannot mediate the autoubiquitination of c-Cbl

Early studies indicated that c-Cbl can ubiquitinate EGFR and Src in cooperation with UbcH7 (32,33), while more recent work showed that c-Cbl promoted EGFR and Src ubiquitination in a UbcH5B dependent fashion (34,35). We tested if c-Cbl can form functional complexes with UbcH7 and/or UbcH5B using an *in vitro* autoubiquitination assay, which is a characteristic commonly used to identify functional E2-E3 pairs (36). To enable accurate

quantitation of ubiquitinated c-Cbl, ^{32}P-Ub-K63 was used in our assays to allow only the mono-ubiquitination of c-Cbl. Figure 1A shows an efficient autoubiquitination of the c-Cbl linker and RING domain (aa 358-437) in the presence of UbcH5B (lanes 4-8). In contrast, UbcH7 was not active in this system even at very high protein concentration (lanes 9-13). These observations confirm the results of more recent studies (34,35) and suggest that the UbcH7/c-Cbl complex might be a nonproductive E2-E3 complex. Similar results were obtained using native ubiquitin allowing poly-ubiquitination (data not shown).

To exclude a possible deficiency in our E2 isolates, we tested the integrity of our E2 enzyme preparations in an E2 activation assay (Figure 1B). Both UbcH5B and UbcH7 showed efficient formation of ubiquitin-thioester linkages. We also tested the E2 specificity of c-Cbl ubiquitination using a larger c-Cbl construct (47-447) that was previously co-crystallized with UbcH7 (5) and observed that UbcH7 failed to support its ubiquitination as well (Figure 1C). Finally, we examined whether UbcH7 and UbcH5B can support the c-Cbl induced ubiquitination of Src, a nonreceptor-type protein tyrosine kinase. Our data show that Src was only ubiquitinated by UbcH5B (Supplementary Figure 1). These data demonstrate that the c-Cbl-UbcH7 complex is a non-productive E2-E3 complex *in vitro*, while under the same conditions the c-Cbl-UbcH5B complex is productive. This indicates that the physical binding between an E2 and an E3 does not suffice for function. We decided to test a number of factors that might explain the different functionality of UbcH5B and UbcH7 complexed to the c-Cbl RING domain.

c-Cbl RING binds to UbcH5B and UbcH7 in a similar fashion

First, we tested the possibility that the two E2s might interact with subtly different c-Cbl protein interfaces. We addressed this question by NMR, because the changes in a [^{1}H, ^{15}N]-HSQC protein spectrum are a very sensitive marker to map interactions with other factors on its protein surface at high resolution. We studied the interaction between E2 enzymes and c-Cbl using ^{15}N-labeled c-Cbl (358-437), which contains both the RING domain and the N-terminal helical linker region previously implicated in E2 binding (5). In the following discussion, c-Cbl refers to c-Cbl (358-437) unless specified otherwise.

To identify differences between UbcH7 and UbcH5B binding to c-Cbl, we recorded a series of [^{1}H-^{15}N]-HSQC spectra of c-Cbl to which increasing amounts of unlabeled UbcH7 and UbcH5B had been added. The c-Cbl backbone amide peaks sensitive to UbcH7 binding belong essentially to the same residues that in the crystal structure have been also found in close proximity to UbcH7 (Figure 2B). The most perturbed residues in the NMR spectra of the complexes occurred in two c-Cbl regions: residues 383-387 in loop L1, and residues 404-420 in the helix H2 and loop L2 of the RING domain. In contrast to the crystal structure, we have no indications of UbcH7 interaction with residues in the c-Cbl linker H1 region. A comparison between the c-Cbl residues implicated in binding to UbcH5B and to UbcH7 shows that both E2s use a very similar protein interface (Figure 2A, C). This data indicates that c-Cbl interacts with UbcH5B and UbcH7 in a highly similar fashion.

The saturation curves for the chemical changes of the two representative residues in c-Cbl upon titration with UbcH5B and UbcH7 were fitted with a 1:1 stoichiometry (Figure 2D) and show that the binding affinity of UbcH7 to c-Cbl was more than 5 times higher than UbcH5B to c-Cbl. The observations, that c-Cbl bound stronger to UbcH7 and that c-Cbl displayed larger resonance shifts upon binding to UbcH7 than to UbcH5B (Figure 2A and 2B),

might be explained by induced conformational changes in the c-Cbl structure that could affect E2 specificity. However, binding of the two E2s to c-Cbl did not cause chemical shift perturbations for residues distant from the E2 binding site, suggesting that no global c-Cbl conformational changes occurred upon binding. To address this question in more detail, we solved the free solution structure of c-Cbl and compared it with the c-Cbl-UbcH7 complex determined by X-ray crystallography.

The c-Cbl RING domain does not show conformational changes upon E2 binding

We obtained a high-resolution solution structure based on 1128 nuclear Overhauser effect (NOE)-derived distance restrains and 58 dihedral angles (Table 2). The RING motif is composed of two large Zn^{2+}-binding loops, a short three-stranded anti-parallel β-sheet and a central α-helix (Figure 3A). The overall structure of the central c-Cbl Ring motif as determined by NMR is very similar to other RING domain structures. A superposition of the free solution structure of the c-Cbl RING domain to that in the X-ray solved UbcH7 complex shows that the structures are highly similar (Figure 3B). One minor difference between both structures is the conformation of Pro395, which resides between β-stand 1 and 2. The NMR data demonstrate it adopts a cis-conformation in solution instead of the trans conformation in the X-ray structure. The linker region also forms a α-helix in solution, but it is not well defined with respect to the rest of the domain. This is probably explained by the absence of the N-terminal TKB domain, which might stabilize this helix by direct interactions with the linker helix H1 Tyr368 and Tyr371 important in c-Cbl phosphorylation (37). Taken together, these data indicate that there is no evidence for a conformational change upon c-Cbl RING binding to UbcH7.

UbcH5B and UbcH7 bind c-Cbl with similar interfaces

Next, we tested if the functional specificity of the E2-E3 complexes could be caused by structural differences in the E2 enzymes upon binding to c-Cbl. We studied the consequences of c-Cbl binding using NMR titration experiments reciprocal to those represented in Figure 2. Unlabeled c-Cbl RING was added stepwise to ^{15}N-labeled UbcH5B and UbcH7 from a 1:5 to a final 2:1 molar ratio. The largest chemical shift perturbations in UbcH5B and UbcH7 were located in the first helix H1, loop L1 between β-strands 3 and 4 and loop L2, connecting β-strand 4 and helix H2 (Figure 4). UbcH7 displayed larger chemical shift changes than UbcH5B, in agreement with our observations on the c-Cbl side (Figure 2). Already at a 1:5 molar ratio of c-Cbl: UbcH7, the majority of the UbcH7 L2 signals disappeared completely. The peaks belonging to L1 residues F63 and K64 disappeared at lower molar ratios, but reappeared and shifted with increasing amounts of c-Cbl. We did not observe significant changes in the proximity of the catalytic cysteine upon c-Cbl binding to UbcH7.

The chemical shift perturbations in UbcH5B observed upon c-Cbl addition were generally less pronounced. Most of the L1 and L2 resonances disappeared when the molar ratio approached 1:1. Some residues with weak peak intensities disappeared upon complex formation, most likely caused by the increased size and lower tumbling rate of the complex. No significant chemical shift changes were observed in the proximity of the catalytic cysteine. In summary, these data suggest that UbcH5B and UbcH7 bind to c-Cbl in a similar fashion, and importantly, there was no evidence that c-Cbl binding induced changes in the catalytic center.

The E2-E3 binding interface does not determine the functional specificity of E2-E3 interaction

Structural and mutagenesis studies of a number

of E2s have identified three regions important for binding to the E3s: the first helix H1, loop L1 and loop L2. Also UbcH5B and UbcH7 interact with the c-Cbl RING domain using these same three regions (Figure 4). The mechanism of the E2-E3 interaction is structurally conserved, but specific E2-E3 pairs use subtle variations of a fundamentally similar interaction interface (5,6,8), which could explain the different consequences of UbcH7 and UbcH5B binding. The Lys-Pro-Ala pattern in UbcH7 loop2 (Table 1) could not be accommodated in the closely packed interface with the U-Box protein CHIP (8), while UbcH5B could since it contains a serine at the position of the lysine, which might result in functionally different outcomes. Furthermore, there are differences in L1 and H1. It is currently disputed whether the specificity of E2s is dependent upon the composition of their L1 and L2. To further characterize the importance of the E3 interaction regions H1, L1 and L2, and test if any of these three regions causes the functional specificity of the E2 for the c-Cbl RING finger, we created three chimeric UbcH5B/UbcH7 proteins (Table 1). In chimera 7H1, we replaced helix H1 of UbcH5B with the helix of UbcH7. Likewise, in the 7L1 and 7L2 mutants, we swapped UbcH5B loops L1 and L2 with the corresponding loops of UbcH7.

First, we confirmed proper folding of the three chimeric proteins with [^{1}H, ^{15}N]-HSQC spectra (Supplementary Figure 3). The HSQC spectra are highly similar for residues not directly neighbouring the substituted motifs, which shows that the mutants adopt highly similar conformations. Second, the chimeras showed a similar ability to bind c-Cbl during HSQC titration (data not shown). Next, we evaluated the chimeras by a number of functional assays. In an E2 activation assay, chimeras 7H1 and 7L1 formed thioester linkages to ubiquitin with UbcH5B wild type like efficiency (Figure 5A, C). Chimera 7L2 possessed slightly weaker E2 activity than wild type UbcH5B. The changes in L2 might induce subtle conformational changes to the catalytic region because of its closer proximity and lower E2 activity. Contrary to expectation, all three chimeras could ubiquitinate c-Cbl with efficiency slight less than that of wild type UbcH5B (Figure 5B, D), while even the lower E2 activation efficiency of 7L2 did not compromise efficient transfer of ubiquitin from 7L2 to c-Cbl. Together, these observations indicate that the inability of UbcH7~Ub to transfer ubiquitin to c-Cbl is not caused by differences in the E2/E3 interaction surface.

The UbcH7~Ub thioester is more stable than UbcH5B~Ub

Since we ruled out both structural changes and subtle differences in the interaction surface as possible explanations for the functional specificity of UbcH5B and UbcH7 in their interaction with c-Cbl, we focused on the intrinsic catalytic properties of the two E2 enzymes. Therefore, we studied the release rate of ubiquitin from activated E2 to different ubiquitin acceptors including H_2O. After charging the E2 with ubiquitin, we assayed the time course of E2~Ub dissociation. By adding apyrase, we can deplete the ATP needed for E1 activity and monitor E2~Ub dissociation in the absence of E2 recharging.

Under recharging conditions, the levels of UbcH5B~Ub and UbcH7~Ub were stable for more than three hours, since E2~Ub formation and dissociation are in equilibrium (Figure 6A). The addition of c-Cbl enhanced the ubiquitin release rate of UbcH5B~Ub, but not of UbcH7~Ub (Figure 6B). When recharging was blocked by the addition of apyrase, UbcH5B~Ub released ubiquitin from its thioester 10 times faster than UbcH7 (Figure 6C and 6E). The addition of c-Cbl slightly slowed down ubiquitin release from UbcH5B (Figure 6C and 6D), In contrast, CNOT4 and Apc2/11 can enhanced the rate of ubiquitin release from UbcH5B~Ub (38).

7

The release rate of ubiquitin from UbcH7~Ub in the absence of recharging was not affected by the presence of c-Cbl (Figure 6E).

The quick release of ubiquitin from UbcH5B~Ub to c-Cbl and water suggests that UbcH5B might be a relatively pliable E2, which could explain why many RING E3s can be ubiquitinated by UbcH5B. We also examined the ubiquitin release rate of the three UbcH5B/UbcH7 chimeras, and found that they behaved like the wild type UbcH5B (supplementary Figure 4B). In contrast, UbcH7~Ub is too stable to release ubiquitin to H_2O under our assay conditions, which indicates that UbcH7 could have a more restricted specificity. This intrinsic stability of the E2~Ub thioester intermediate is unique for each E2, which suggests that understanding the factors that influence E2~Ub thioester stability will help to understand E2 specificity.

Stronger binding between UbcH7 and c-Cbl RING does not protect c-Cbl from ubiquitination by UbcH5B

UbcH7 was unable to transfer ubiquitin to c-Cbl in the *in vitro* autoubiquitination assay despite its ability to bind the same surface of c-Cbl RING as UbcH5B. In our experiments, we found that UbcH7 can even bind stronger to c-Cbl RING than UbcH5B, which raises the possibility that UbcH7 might protect c-Cbl from ubiquitination by competing with UbcH5B binding. Ubiquitin transfer assays were used to assess if pre-incubation of c-Cbl with UbcH7 influences the amount of ubiquitin transferred to c-Cbl. Thus, c-Cbl RING was preincubated with different amounts of UbcH7 and these mixtures were added to reactions in which 4μM UbcH5B had been charged with ubiquitin (Figure 7). Samples were taken out at indicated timepoints to compare the level of ubiquitinated c-Cbl in the reactions. Interestingly, pre-incubation of c-Cbl with UbcH7 did not affect its level of ubiquitination (Figure 7D), indicating that the

stronger binding between UbcH7 and c-Cbl will not prevent c-Cbl from ubiquitination by activated UbcH5B. Taken together, the results presented here indicate that substrate specificity in the ubiquitination pathway is not solely determined by the specificity of E2-E3 interactions, but intrinsic enzymatic differences between E2 enzymes can play an additional key role in substrate ubiquitination.

Discussion

In our experiments, we found that only UbcH5B can support the *in vitro* ubiquitination of c-Cbl and c-Cbl-facilitated substrate ubiquitination. NMR titrations of c-Cbl to UbcH5B and UbcH7 did not show structural distinctions that could explain the functional differences. More likely, the different stability of the thioesters UbcH5B~Ub and UbcH7~Ub might explain why c-Cbl/UbcH7 is "nonproductive" *in vitro*. The E2~Ub thioester intermediate is a key intermediate in the ubiquitination pathway, in which it is the E2~Ub, but not the E2 itself, that interacts and functions with E3 and substrate. Unfortunately, the transient nature of this thioester makes it very difficult to study its interactions with E3. The NMR study of the formation of S22R-UbcH5C~Ub thioester showed that chemical shift perturbations on UbcH5C were not solely a consequence of direct contact with Ub, but also induced by allosteric effects (4), which might explain the different properties of E2~Ub and E2 in their interaction with E3 or substrate.

Electrostatic potentials of UbcH5b and UbcH7

A comparison of the electrostatic potential surface of UbcH7 and UbcH5B reveals striking differences (Figure 8). Protein Interaction Property Similarity Analysis (PIPSA) is a measure of electrostatic potential similarity and ranges from -1 on full anti-correlation to 1 on perfect correlation between two potentials (39).

Autoubiquitination of BRCA1 could be facilitated by Ube2w, UbcH6 and UbcH5, but not by UbcH7 (40). UbcH5B has much less electrostatic potential similarity to UbcH7 (0.394) than it has to UbcH6 (0.678) and Ube2w (0.613). The biggest difference in electrostatic potential between UbcH5B and UbcH7 is observed at the β-sheet implicated in noncovalent ubiquitin binding (Figure 8), which corresponds to the fact that only UncH5B can noncovalent bind to ubiquitin (4). Interestingly, the E2~Ub thioester interfaces of UbcH5B and UbcH7 also display differences: although both are negatively charged, UbcH7 is more negatively charged both close to the catalytic cysteine as well as at the residues expected to bind Ub upon thioester formation (9). The increased stability of the UbcH7~Ub thioester might be explained by this superior complementarity to the positively charged Ub thioester interface.

Functional specificity of UbcH5B and UbcH7

The intrinsic high stability of the UbcH7~Ub thioester intermediate could explain why UbcH7 fails to transfer ubiquitin to c-Cbl, but also suggests that other accessory factors might be needed to help the release of ubiquitin from UbcH7~Ub thioester to its substrates or E3. For example, the auxiliary protein Smad7 can recruit UbcH7 to the HECT E3 Smurf2, and regulates the catalytic activity of Smurf2 at the level of E2 recognition (20). Ubiquitination of Trk by UbcH7 and the TRAF6/E3 was carried out in the presence of p75 and p62 (41).

Although the E3 interacts with E2 on the common interface composed of helix H1, loop L1 and loop L2, E3s have their own preference for the binding position on E2s. For example, K63 of UbcH5b, F63 of UbcH7 and M64 of Ubc13 in loop L1 were important in the interactions with CNOT4, c-Cbl and CHIP respectively (5,8,23), while the loop L2 residues of UbcH5C showed bigger perturbations upon binding to BRCA1-BARD1 (40). The mechanism underlying the E2-E3 interactions and functions is not well understood, but it seems that dynamic, transient and modest affinity interactions are more productive. Similarly as observed for the BRCA1/BARD1, the stronger binding of c-Cbl to UbcH7 did not facilitate ubiquitin transfer. Also, in the case of E6AP/UbcH7, there was no correlation between the increased formation of ubiquitin-E6AP and enhanced binding affinity of UbcH7 and mutant E6AP (42). These results imply that the ubiquitination pathway might not be optimized for one particular pairwise interaction, but is rather designed to function in its entirety (43). Together with our comparison of UbcH5B and UbcH7 in c-Cbl ubiquitination, this indicates that binding specificity only compromises a part of the functional specificity of E2 enzymes. In addition, intrinsic enzymatic differences between E2 enzymes can play a key role in substrate ubiquitination. Does the binding specificity of E2-E3s form the basis for their functional specificity? We believe the answer is yes, although the physical interaction between a functional E2-E3 pair is required, yet not necessarily sufficient to transfer ubiquitin to substrates.

References

1. Pickart, C. M. (2001) *Annu Rev Biochem* 70, 503-533
2. Kerscher, O., Felberbaum, R., and Hochstrasser, M. (2006) *Annu Rev Cell Dev Biol* 22, 159-180
3. Andersen, P. L., Zhou, H., Pastushok, L., Moraes, T., McKenna, S., Ziola, B., Ellison, M. J., Dixit, V. M., and Xiao, W. (2005) *J Cell Biol* 170, 745-755
4. Brzovic, P. S., Lissounov, A., Christensen, D. E., Hoyt, D. W., and Klevit, R. E. (2006) *Mol Cell* 21, 873-880
5. Zheng, N., Wang, P., Jeffrey, P. D., and Pavletich, N. P. (2000) *Cell* 102, 533-539
6. Huang, L., Kinnucan, E., Wang, G., Beaudenon, S., Howley, P. M., Huibregtse, J. M., and Pavletich, N. P. (1999) *Science* 286, 1321-1326
7. Dominguez, C., Bonvin, A. M., Winkler, G. S., van Schaik, F. M., Timmers, H. T., and Boelens, R. (2004) *Structure* 12, 633-644
8. Zhang, M., Windheim, M., Roe, S. M., Peggie, M., Cohen, P., Prodromou, C., and Pearl, L. H. (2005) *Mol Cell* 20, 525-538
9. Hamilton, K. S., Ellison, M. J., Barber, K. R., Williams, R. S., Huzil, J. T., McKenna, S., Ptak, C., Glover, M., and Shaw, G. S. (2001) *Structure* 9, 897-904
10. Jin, J., Li, X., Gygi, S. P., and Harper, J. W. (2007) *Nature* 447, 1135-1138
11. Glickman, M. H., and Ciechanover, A. (2002) *Physiol Rev* 82, 373-428
12. Kus, B. M., Caldon, C. E., Andorn-Broza, R., and Edwards, A. M. (2004) *Proteins* 54, 455-467
13. Petroski, M. D., and Deshaies, R. J. (2005) *Cell* 123, 1107-1120
14. Jin, L., Williamson, A., Banerjee, S., Philipp, I., and Rape, M. (2008) *Cell* 133, 653-665
15. Kirkpatrick, D. S., Hathaway, N. A., Hanna, J., Elsasser, S., Rush, J., Finley, D., King, R. W., and Gygi, S. P. (2006) *Nat Cell Biol* 8, 700-710
16. Brzovic, P. S., Keeffe, J. R., Nishikawa, H., Miyamoto, K., Fox, D., 3rd, Fukuda, M., Ohta, T., and Klevit, R. (2003) *Proc Natl Acad Sci U S A* 100, 5646-5651
17. Buchwald, G., van der Stoop, P., Weichenrieder, O., Perrakis, A., van Lohuizen, M., and Sixma, T. K. (2006) *EMBO J* 25, 2465-2474
18. Peschard, P., Kozlov, G., Lin, T., Mirza, I. A., Berghuis, A. M., Lipkowitz, S., Park, M., and Gehring, K. (2007) *Mol Cell* 27, 474-485
19. Joazeiro, C. A., Wing, S. S., Huang, H., Leverson, J. D., Hunter, T., and Liu, Y. C. (1999) *Science* 286, 309-312
20. Ogunjimi, A. A., Briant, D. J., Pece-Barbara, N., Le Roy, C., Di Guglielmo, G. M., Kavsak, P., Rasmussen, R. K., Seet, B. T., Sicheri, F., and Wrana, J. L. (2005) *Mol Cell* 19, 297-308
21. Gallagher, E., Gao, M., Liu, Y. C., and Karin, M. (2006) *Proc Natl Acad Sci U S A* 103, 1717-1722
22. de Jong, R. N., Daniels, M. A., Kaptein, R., and Folkers, G. E. (2006) *J Struct Funct Genomics* 7, 109-118
23. Albert, T. K., Hanzawa, H., Legtenberg, Y. I., de Ruwe, M. J., van den Heuvel, F. A., Collart, M. A., Boelens, R., and Timmers, H. T. (2002) *EMBO J* 21, 355-364

24. Folkers, G. E., van Buuren, B. N., and Kaptein, R. (2004) *J Struct Funct Genomics* 5, 119-131

25. Sattler, M., Schleucher, J., and Griesinger, C. (1999) *Progress in Nuclear Magnetic Resonance Spectroscopy* 34, 93-158

26. Herrmann, T., Guntert, P., and Wuthrich, K. (2002) *J Mol Biol* 319, 209-227

27. Vriend, G. (1990) *J Mol Graph* 8, 52-56, 29

28. Morris, A. L., MacArthur, M. W., Hutchinson, E. G., and Thornton, J. M. (1992) *Proteins* 12, 345-364

29. DeLano, W. (2002) *San Carlos, CA, USA DeLano Scientific*

30. Houben, K., Dominguez, C., van Schaik, F. M., Timmers, H. T., Bonvin, A. M., and Boelens, R. (2004) *J Mol Biol* 344, 513-526

31. Serniwka, S. A., and Shaw, G. S. (2007) *Biomolecular NMR Assignments*

32. Yokouchi, M., Kondo, T., Houghton, A., Bartkiewicz, M., Horne, W. C., Zhang, H., Yoshimura, A., and Baron, R. (1999) *J Biol Chem* 274, 31707-31712

33. Yokouchi, M., Kondo, T., Sanjay, A., Houghton, A., Yoshimura, A., Komiya, S., Zhang, H., and Baron, R. (2001) *J Biol Chem* 276, 35185-35193

34. Levkowitz, G., Waterman, H., Ettenberg, S. A., Katz, M., Tsygankov, A. Y., Alroy, I., Lavi, S., Iwai, K., Reiss, Y., Ciechanover, A., Lipkowitz, S., and Yarden, Y. (1999) *Mol Cell* 4, 1029-1040

35. Kim, M., Tezuka, T., Tanaka, K., and Yamamoto, T. (2004) *Oncogene* 23, 1645-1655

36. Lorick, K. L., Jensen, J. P., Fang, S., Ong, A. M., Hatakeyama, S., and Weissman, A. M. (1999) *Proc Natl Acad Sci U S A* 96, 11364-11369

37. Thien, C. B., and Langdon, W. Y. (2005) *Biochem J* 391, 153-166

38. Ozkan, E., Yu, H., and Deisenhofer, J. (2005) *Proc Natl Acad Sci U S A* 102, 18890-18895

39. Winn, P. J., Zahran, M., Battey, J. N., Zhou, Y., Wade, R. C., and Banerjee, A. (2007) *Front Biosci* 12, 3419-3430

40. Christensen, D. E., Brzovic, P. S., and Klevit, R. E. (2007) Nat Struct Mol Biol 14, 941-948

41. Geetha, T., Jiang, J., and Wooten, M. W. (2005) Mol Cell 20, 301-312

42. Eletr, Z. M., and Kuhlman, B. (2007) J Mol Biol 369, 419-428

43. Huang, D. T., Zhuang, M., Ayrault, O., and Schulman, B. A. (2008) Nat Struct Mol Biol 15, 280-287

Footnotes

The abbreviations used are: E1, ubiquitin-activating enzyme; E2, ubiquitin-conjugating enzyme; E3, ubiquitin-protein ligase; Ub, ubiquitin; Ub-K63, ubiquitin with all lysine residues were mutated except for K63

Acknowledgements

Legends

Figure 1. **UbcH7 does not support autoubiquitination of c-Cbl.** Ubiquitin modification via isopeptide bonds resists DTT treatment and is indicated as –Ub, while ubiquitin modification via thioester linkages is sensitive to DTT and denoted with ~Ub. (A) Autoubiquitination of c-Cbl linker and RING domain (358-437) with UbcH5B and UbcH7. E3 ligation assays were performed using increasing amounts of E2 enzyme and a radiolabeled ubiquitin mutant incapable of K48 linked polyubiquitin chain formation. Reaction products were separated by reducing SDS-PAGE. (B) Activation of UbcH5B and UbcH7. E2 ubiquitin conjugation assays of UbcH5B and UbcH7 were performed at increasing E2 concentrations, in the absence of E3 ligase; reaction products were separated using non-reducing SDS-PAGE. Activity of purified UbcH5B and UbcH7 is confirmed by the formation of thioester intermediates, indicated as UbcH5B~Ub and UbcH7~Ub. (C) Autoubiquitination of c-Cbl TKB and RING domain (47-447) with UbcH5B and UbcH7. E3 ligation assay products were analyzed by reducing SDS-PAGE.

Figure 2. **Mapping of c-Cbl RING amino acids implicated in binding with UbcH5B and UbcH7.** Unlabeled UbcH5B (panel A) or UbcH7 (panel B) was titrated into ^{15}N-c-Cbl (358-437) to a final E3:E2 ratio of 1:1.5, and NMR chemical shift changes were recorded. NMR peaks for residue names colored orange were missing or disappeared during titration. Dotted lines indicate chemical shift perturbation threshold (0.08ppm for UbcH5B, 0.12ppm for UbcH7) (C) UbcH5B (top) and UbcH7 (bottom) chemical shift perturbations mapped on the c-Cbl crystal structure (PDB ID: 1FBV). Chemical shift changes are colored from white to red (maximal shift). Sidechains colored black indicate signals that were missing or disappeared during titration. (D) Chemical shift perturbations of c-Cbl I383 and S411 fitted to standard 1:1 binding curves.

Figure 3. **NMR solution structure of c-Cbl linker and RING domain (358-437).** (A) Free NMR solution structure of c-Cbl linker and RING domain. (B) Free NMR solution structure of c-Cbl RING finger domain (lime) superimposed on the crystal structure of the c-Cbl RING finger domain (grey) complexed to UbcH7 (PDB ID: 1FBV).

Figure 4. **UbcH5B and UbcH7 interaction surfaces with c-Cbl mapped by NMR chemical shift perturbation.** ^{15}N-labeled UbcH5B (panel A) and UbcH7 (panel B) were incubated with increasing amounts of unlabeled c-Cbl (358-437). UbcH5B (panel C) and UbcH7 (panel D) NMR chemical shift perturbations upon c-Cbl addition were mapped on their respective structures (PDB ID: 1W4U and 1FBV). Chemical shift changes are colored from white (below threshold of 0.05 ppm) to red (maximal). Sidechains colored black indicate signals that were missing or disappeared during titration. The catalytic cysteine is indicated in yellow.

Figure 5. **Analysis of the E2/E3 interaction surface using chimeric UbcH5B/UbcH7 proteins.** (A) E2 conjugation assays (see legend to Figure 1B) of the three chimeras 7H1, 7L1 and 7L2. The activity of these three chimeras was confirmed by the formation of thioester intermediates indicated as E2~Ub. (B) Autoubiquitination activity assays (see legend to Figure 1) of c-Cbl RING domain by the three chimeric E2 enzymes 7H1 7L1 and 7L2. All three chimeras can support c-Cbl RING autoubiquitination with an efficiency similar to that of wild type UbcH5B. E2-Ub and c-Cbl-Ub are indicated. (C) Quantitation of reactions shown in panel A. 7L2 had weaker E2 enzyme activity. (D) Quantitation of reactions shown in panel B.

Figure 6. **Ubiquitin thioester stability measurements.** (A) UbcH5B or UbcH7 were charged with ubiquitin by incubating with E1, ubiquitin, and ATP for 30 minutes. Subsequently, samples were taken at the indicated time points and separated using non-reducing SDS-PAGE. (B) After a 30 min preincubation as described for (A), c-Cbl was added at the start of the sampling timecourse. (C) After the 30 min preincubation as described for (A), apyrase was added at the start of the sampling timecourse to deplete ATP and block E1-dependent ubiquitin charging of E2. (D) As described in (C) with addition of c-Cbl at the start of the sampling timecourse. (E) Quantitation of reactions shown in panel C and panel D. The upper 2 lines are the timecourses of UbcH7~Ub amount without and with addition of c-Cbl RING. The lower 2 lines are the timecoures of UbcH5B~Ub amount with and without addition of c-Cbl RING.

Figure 7. **UbcH7 does not protect c-Cbl from ubiquitination by UbcH5B.** c-Cbl was preincubated with 0 μM (A) 4μM (B) or 8 μM (C) UbcH7, while UbcH5B was activated separately in the presence of E1, ubiquitin and ATP. After mixing the two premixes, samples were taken out at the indicated timepoints. (D) Quantitation of reactions shown in panels A, B and C. Similar amounts of c-Cbl-Ub were formed in these 3 reactions.

Figure 8. **Comparison of surface properties of UbcH5B and UbcH7.** (A) Top: electrostatic surface potential of UbcH5B was calculated using the APBS plugin to PyMol and indicated as a charge scale from negative -1 (red) to positive +1 (blue). Bottom: surface representation of interaction sites on Ubch5B. The catalytic site (yellow), E2~Ub binding interface (cyan), E3 binding interface (orange), and the non-covalent Ub-binding interface on UbcH5B (green) are indicated. (B) UbcH7 electrostatic surface potential (top) and interaction sites (bottom), colored as indicated under (A).

Table1. **E3 interaction motifs in UbcH5B, UbcH7 and three chimeric proteins.**

	helix H1	loop L1	loop L2
UbcH5B	MALKRIHKELNDLARD	FPTDYPFKPP	QWSPALTI
UbcH7	**MAASRRLMKELEEIRKC**	**FPAEYPFKPP**	**NWKPATKT**
7H1	**MAASRRLMKELEEIRKC**	FPTDYPFKPP	QWSPALTI
7L1	MALKRIHKELNDLARD	**FPAEYPFKPP**	QWSPALTI
7L2	MALKRIHKELNDLARD	FPTDYPFKPP	**NWKPATKT**

Table 2. **Structural statistics of the c-Cbl (358-437) structure ensemble**

Structural statistics for the human c-Cbl RING domain (358-437)

Number of NMR restraints used in the structure calculation

Short-range (|i-j|<=1	669
Medium-range(1<|i-j|<5)	135
Long-range(|i-j|>=5)	324
Total NOE restraints	1128
Phi+psi dihedral restraints	58

Coordinated RMSD from mean(Å)residues 377-430

All backbone atoms	0.5
All heavy atoms	1.0

WHATCHECK

1ST generation packing quality	-2.37
2nd generation packing quality	-0.97
Ramachandran plot appearance	-3.05
chi-1/chi-2 rotamer normality	-0.82
Backbone conformation	-5.16
Number of bumps per 100 residues	32.32

PROCHECK

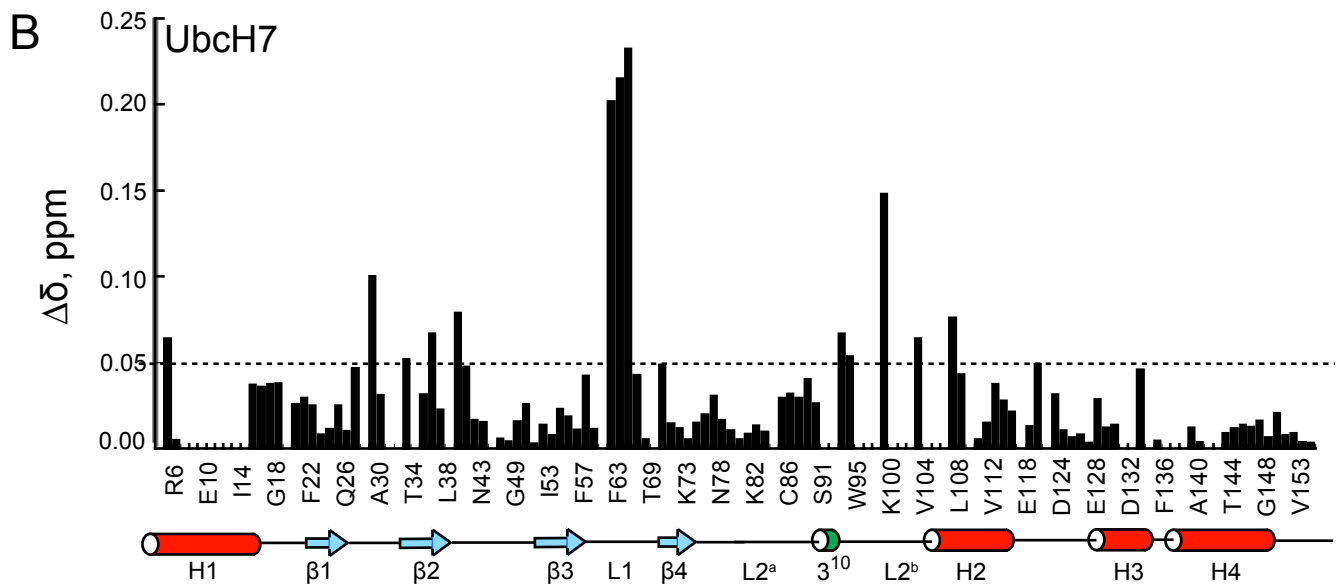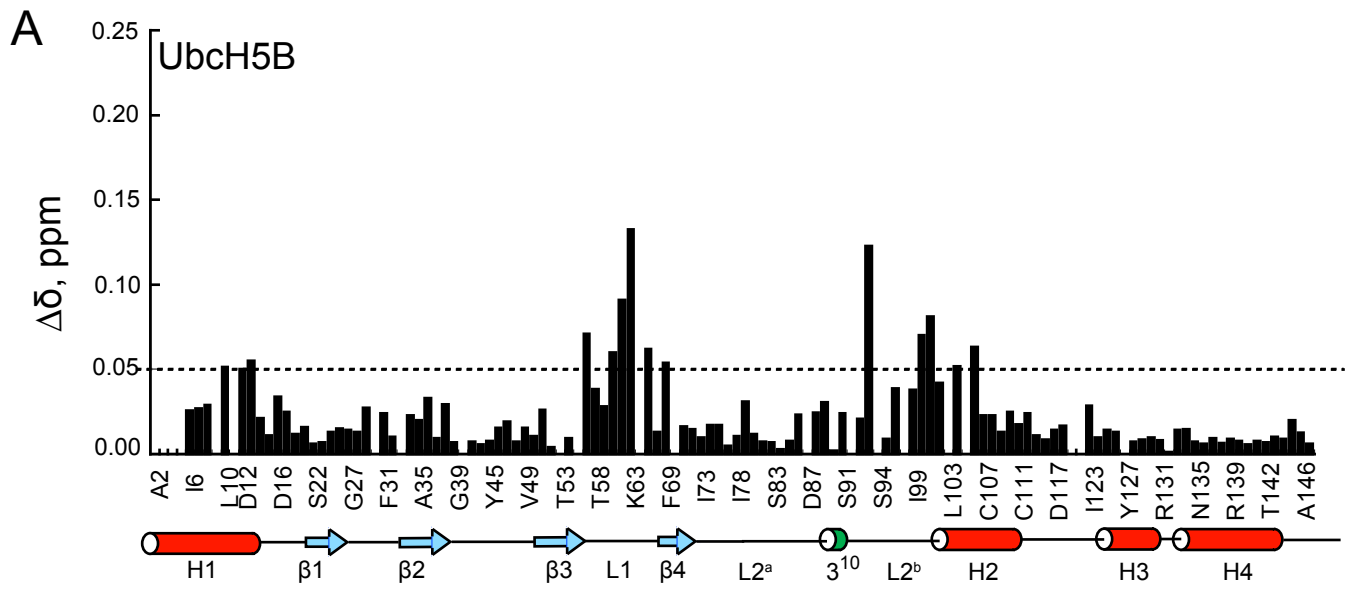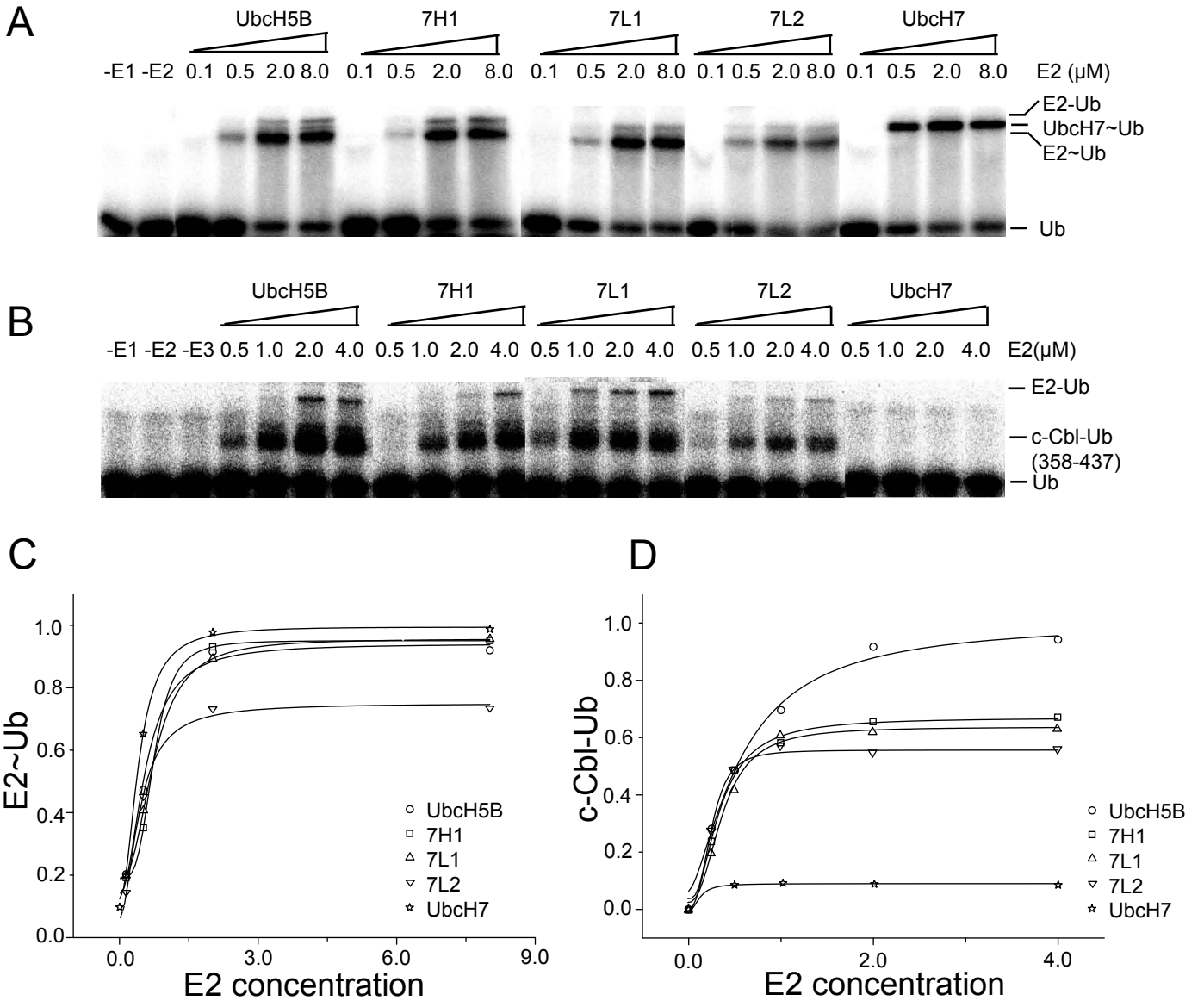|	
Most favored regions	78.9
Allowed regions	19.1
Generously allowed regions	1.4
Disallowed regions	0.6

Figure 1
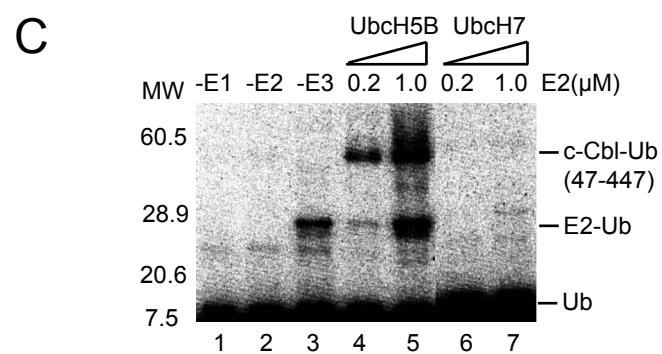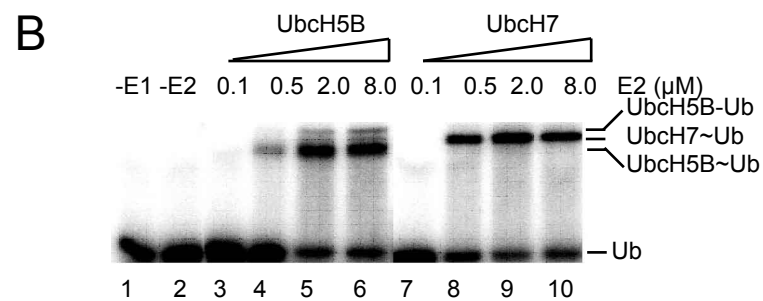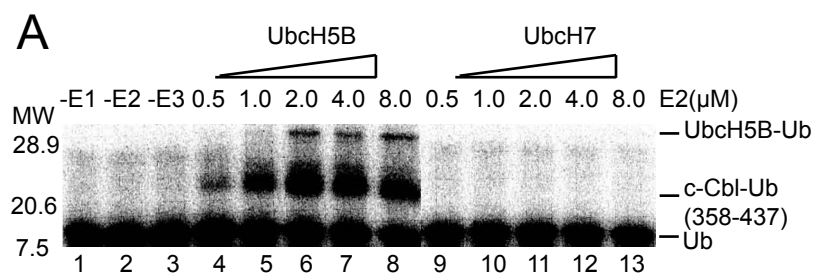
Figure 2
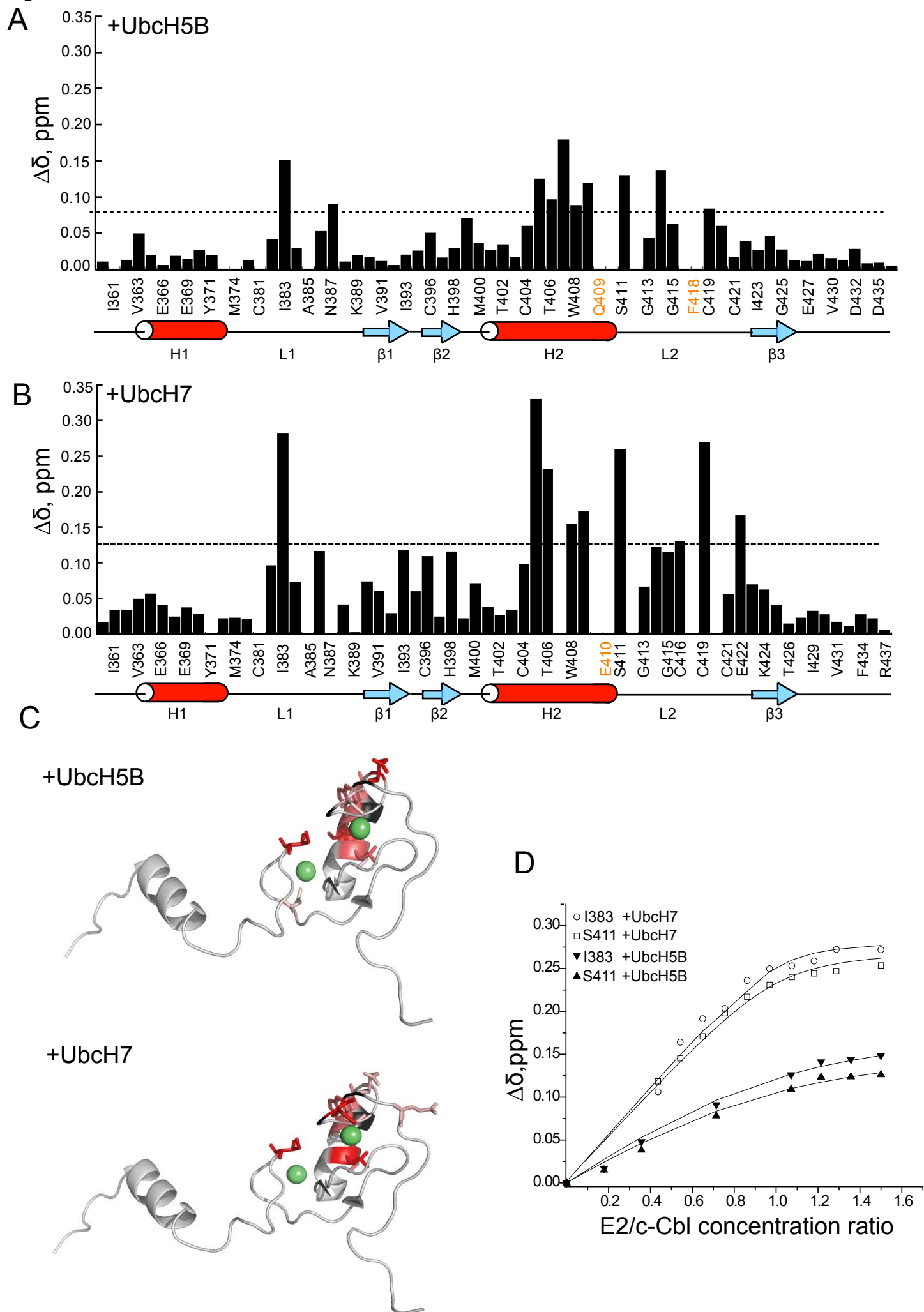
Figure 3
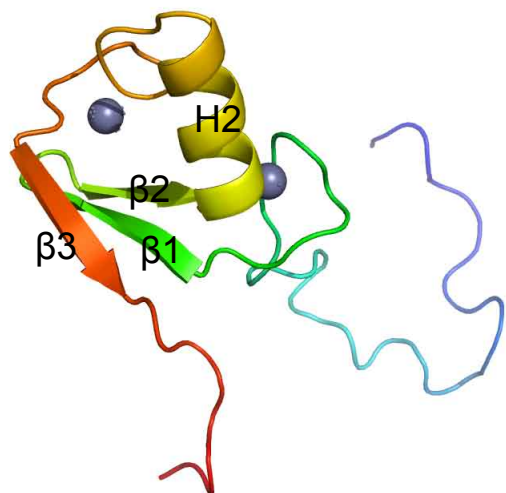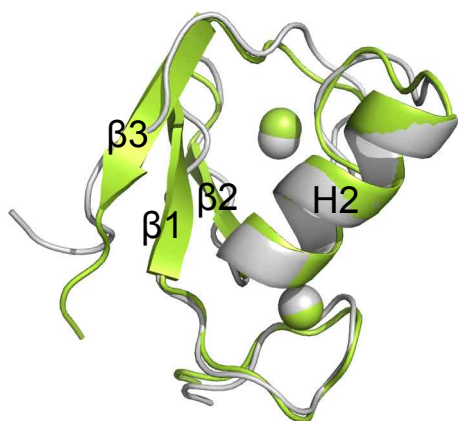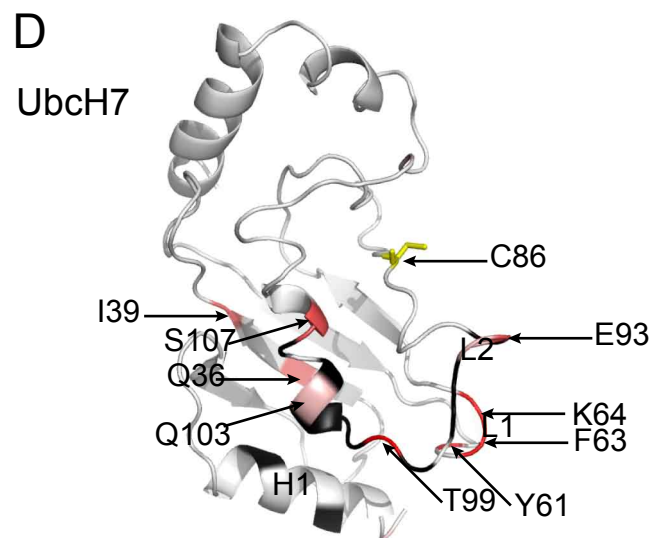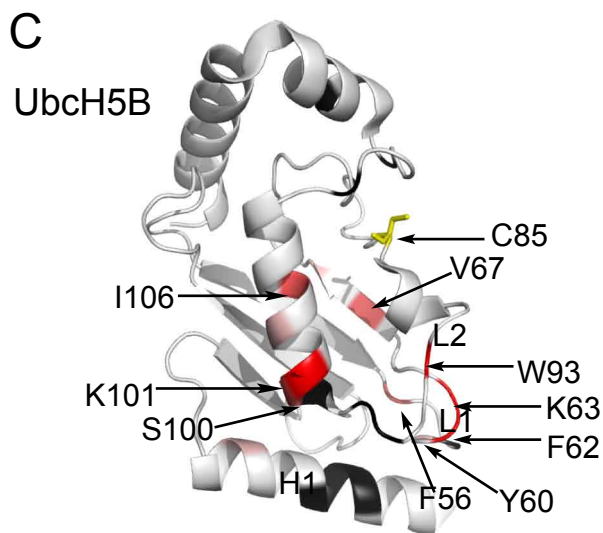
Figure 4

Figure 5

Figure 6

Figure 7

Figure 8

A UbcH5B

a)

C85

b)

E2~Ub interface   C85

E3 binding interface

Ub noncovalent binding

B UbcH7

a)

C86

b)

E2~Ub interface   C86

E3 binding interface

Ub noncovalent binding